Nanotechnology **19** (2008) 505605 (7pp) doi:10.1088/0957-4484/19/50/505605

Engineering of 3D self-directed quantum dot ordering in multilayer InGaAs/GaAs nanostructures by means of flux gas composition

P M Lytvyn[1,2], Yu I Mazur[1], E Marega Jr[1,3], V G Dorogan[1], V P Kladko[2], M V Slobodian[2], V V Strelchuk[2], M L Hussein[1], M E Ware[1] and G J Salamo[1]

[1] Department of Physics, University of Arkansas, Fayetteville, AR 72701, USA
[2] V. Lashkaryov Institute of Semiconductor Physics, NAS of Ukraine, Kiev 03028, Ukraine

E-mail: ymazur@uark.edu

Received 8 September 2008, in final form 25 October 2008
Published 25 November 2008
Online at stacks.iop.org/Nano/19/505605

Abstract
Lateral ordering of InGaAs quantum dots on the GaAs (001) surface has been achieved in earlier reports, resembling an anisotropic pattern. In this work, we present a method of breaking the anisotropy of ordered quantum dots (QDs) by changing the growth environment. We show experimentally that using As_2 molecules instead of As_4 as a background flux is efficient in controlling the diffusion of distant Ga adatoms to make it possible to produce isotropic ordering of InGaAs QDs over GaAs (001). The control of the lateral ordering of QDs under As_2 flux has enabled us to improve their optical properties. Our results are consistent with reported experimental and theoretical data for structure and diffusion on the GaAs surface.

(Some figures in this article are in colour only in the electronic version)

1. Introduction

To date there has been extensive research devoted to fabrication of self-assembled quantum dots (SAQDs) via the Stranski–Krastanov growth mode [1]. The incorporation of quantum dots (QDs) in various devices has been subsequently found to result in large improvements in performance (e.g., of quantum dot lasers, detectors and photonic crystals) [2, 3]. However, in order to use these SAQDs in large-scale integrated devices a high degree of size and shape uniformity and control over spatial positioning of the quantum dots (QDs) is required [4]. Vertical ordering of dots is achieved in multilayer structures provided the thickness of the 'spacer layer' (barrier layer) is similar to the lateral dimension of individual dots [5, 6]. This is due to the elastic interaction of the strained SAQDs during the epitaxial growth of quantum dot multilayer structures and can lead to both improved size uniformity and a lateral ordering of dots, which results in the possibility of realizing long-range correlation in the electronic structure of the dot assembly [7, 8]. Ideally desired is a periodic superstructure of uniform QDs, but this has not yet been achieved. Usually, the Stranski–Krastanov (SK) growth of InGaAs QDs on GaAs(100) is limited in device applications due to randomly distributed QDs on a plane within a structure [9]. While recent approaches using lithographic techniques have demonstrated successful lateral ordering of QDs [10–12], these methods require expensive processing steps, which also introduce possible defects that can also prevent successful application.

In an effort to overcome some of the difficulties inherent to the lateral and vertical ordering of InGaAs QDs on the GaAs (001) surface, the authors have recently investigated using the technique of self-assembly through vertical stacking of QDs with a growth at relatively high temperatures [13]. For example, 'chains' of ordered QDs have been fabricated using this approach [14–16]. Effective 3D ordering of QDs has been demonstrated over high-index surfaces [17], where regular

[3] Permanent address: Instituto de Fisica de Sao Carlos, Universidade de São Paulo, CP 369, São Carlos–SP, CEP–13560-970, Brazil.

surface meshes of different unit cell sizes were grown. All of the above mentioned self-assembled QD's become ordered due to the interacting strain fields of successive QD layers and surface diffusion.

It is apparent that new possibilities in 3D self-directed QD ordering could be achieved if strain and anisotropic diffusion can be controlled separately. One of the known effective ways to change surface diffusion is the deposition of a few monolayers (MLs) of another material on a growth surface [18] or a change in the source gas composition [19]. Improvement of InAs QDs optical properties was reported, where As_2 flux was used instead of usual As_4 [20, 21], but differences in physical processes of lateral and vertical QDs ordering were not under investigations.

In this paper, we report on experiments that use either As_4 or As_2 as the arsenic source gas for growth of InGaAs/GaAs QD superlattices to study the role of both surface diffusion and elastic strain in the formation and development of 3D ordering of the QDs in a GaAs matrix. In particular, our findings show an influence of As flux type on multilayered growth of (In, Ga)As QDs on GaAs (100). This provides an excellent opportunity to vary and control the symmetry of the diffusion and strain pattern in each layer with the aim to optimize the spatial ordering of nanostructures with identical sizes and shapes in multilayers of QDs. This influence of changing the As species during growth on the size distributions and 3D patterns of ordering of the QDs and on the PL spectra was analyzed.

2. Experiments

The InGaAs QDs were grown by molecular beam epitaxy (MBE) on semi-insulating GaAs (100) substrates. Following a 0.3 μm GaAs buffer layer grown at 580 °C to smooth the surface, the growth of InGaAs QDs capped by 60 MLs of GaAs was repeated for a 15 layers superlattice grown at 540 °C. A final QD layer was growth and left uncapped for morphology analysis. Two different species of arsenic were used as sources, As_4 and As_2, which was produced by cracking As_4 molecules at 900 °C. The V/III ratio of the beam equivalent pressure was kept at 15:1 in both cases in order to supply sufficient As atoms so that the growth always proceed in a strongly group III limited regime. For each As species three sets of QD samples were grown using $In_xGa_{1-x}As$ where x was equal to 0.3, 0.4, and 0.5 with nominal thicknesses of 15.5, 8.5 and 5.7 MLs respectively. These thicknesses were chosen to be 25% above the critical thickness for 2D to 3D transition for each composition. Growth interrupts were introduced during the InGaAs layer growth to enhance the surface migration of available adatoms.

The QD growth was monitored by *in situ* reflection high energy electron diffraction. Following the growth, surface morphologies of the samples were analyzed by atomic force microscopy (AFM) to uncover distributions in the shape, size, and lateral arrangement of the QDs. Lateral and vertical ordering of the QDs, as well as residual strain was investigated by high-resolution x-ray reciprocal space mapping. PL measurements were performed at 10–300 K under low intensity excitation by continuous wave YAG laser (wavelength of 532 nm) in order to understand the optical quality of the superlattices.

3. Results and discussion

It is well known that for our growth conditions the maximum sticking coefficient is only 0.5 for As_4, but can reach 1.0 for As_2. However, for sufficient overpressure of As with these same growth conditions, the sticking coefficient for Ga and In is very readily 1.0 [22]. Therefore, the amount of material grown is completely determined by the group III flux. So, it is left up to the group V flux to affect changes in the surface diffusivity of the group III atoms resulting in the many observed, distinct quantum dot structures. Figure 1 shows AFM topographic images of single layers and multilayers for $x = 0.4$, which were grown under As_4 and As_2 fluxes. QDs in the single layer structures have weak lateral ordering for both As_4 and As_2 fluxes (figures 1(a) and (b)). However, it is apparent, that the sample grown using As_2, figure 1(b), is already more uniform and somewhat more ordered than the one using As_4, figure 1(a), after just the first layer. It can be seen that a small fraction of the QDs are positioned in chains along the $[0\bar{1}1]$ crystallographic direction for the first layer of the As_2 sample. After further growth, completing the full 15 period structure, well defined periodic dot-chains are observed (figures 1(c) and (d)) for both As_4 and As_2 growth (figures 1(c) and (d)). The anisotropic surface diffusion coupled with the interlayer strain relaxation of the InGaAs layers determines this organization of the QDs on the final surface [14, 15]. At the same time, it is found that the use of either As_4 or As_2 during the growth causes significant differences in density and size of the QDs. The QD density goes up by a factor of two when using As_4 as compared to As_2. From analysis of figure 1, it is found that the densities of the QDs on the surface are 420 and 280 dots μm^{-2} for use of As_4 and As_2, respectively in the single layer structures and are 280 and 140 dots μm^{-2} for use of As_4 and As_2, respectively in the multilayer structures. A trend is also found in the average diameters of the QDs. The insets of figures 1(a)–(d) show the averaged cross-sectional profiles of the QDs along [011] direction. The As_4-grown QDs are smaller in each case than similarly grown QDs using As_2 where the average height and diameter remains practically the same from first to the 16th layer. These data imply a generally higher surface mobility for QD growth using As_2 as compared to As_4.

To reinforce this idea that the As_2 grown QDs achieve a higher degree of order than the As_4 grown QDs starting with the first layer, we perform 2D fast Fourier transforms (FFT) of the 3 μm × 3 μm AFM data, figure 2. For the single layer structures, these FFTs exhibit two broad bow-shaped maxima for As_4 (figure 2(a)) and sharp (in [011] direction) and broad (in $[0\bar{1}1]$) pairs of maxima for As_2 grown structures. Corresponding cross-sections are shown in the figure 2(e) where the curve 2 shows narrower maximum at 95 nm for As_2 grown sample instead of broad maximum at 65 nm for the As_4 grown one. We found that for multilayer structures the width of FFT peaks (e.g., degree of QDs ordering in [011]

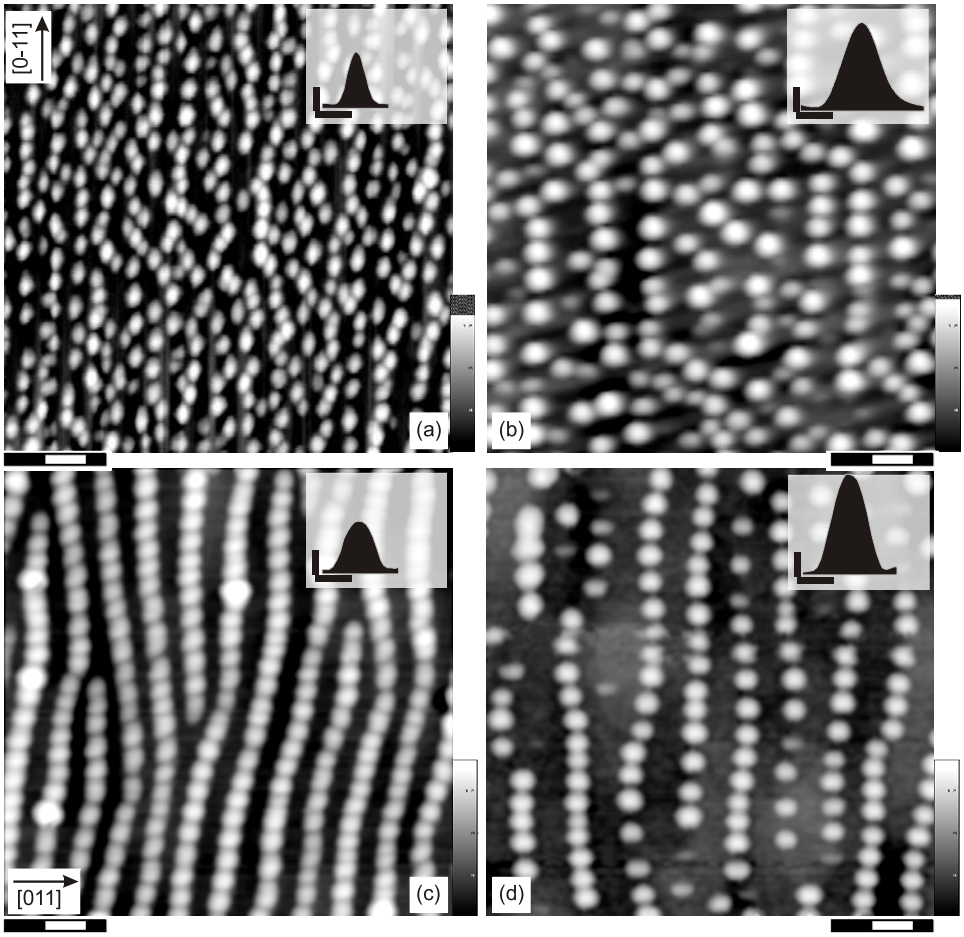

Figure 1. AFM images of the $In_{0.4}Ga_{0.6}As$ QD's on single layer structures ((a), (b)) and 15.5 period structures ((c), (d)) grown using As_4 ((a), (c)) and As_2 ((b), (d)) background fluxes under identical conditions. Insertions in (a)–(d) show the cross-sections (linear profiles) along the [011] direction of most typical QDs determined from size distribution functions (vertical and horizontal scale bars correspond to 6 and 40 nm). Horizontal scale bar corresponds to 250 nm, height gray-color scale corresponds to 15 nm.

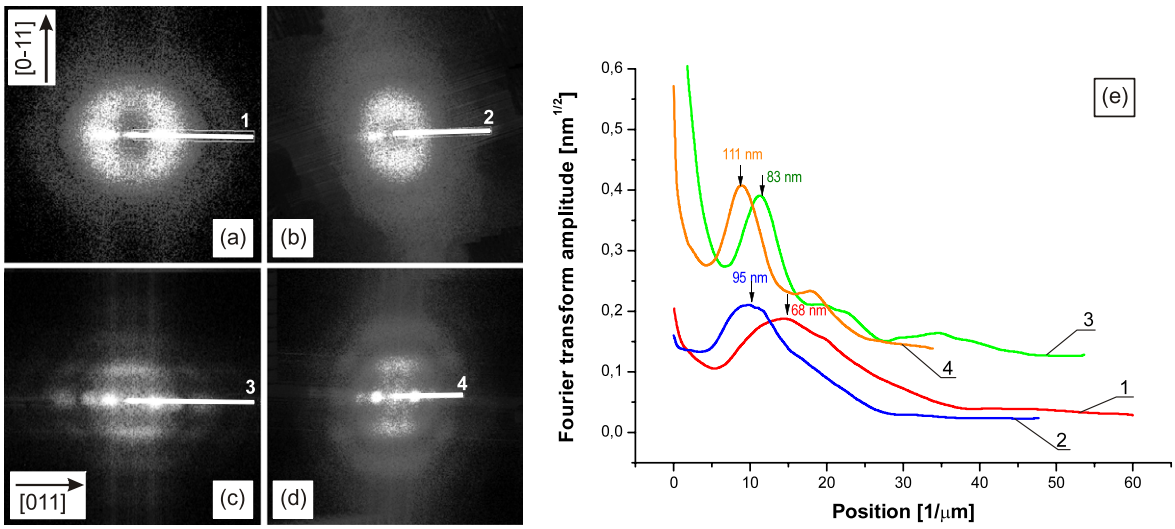

Figure 2. FFTs of AFM data from $In_{0.4}Ga_{0.6}As/GaAs$ structures in figure 1: single layer structures grown using As_4 (a) and As_2 (b) fluxes; 15.5 period structures (c) and (d). Cross-sections of corresponding 2D FFTs (e) along showed lines. Cross-sections 3 and 4 are shifted up to 0.1 $nm^{1/2}$ for better visualization. (FFT's size is 2 μm^{-1} × 63.7 μm^{-1}. FFTs were calculated from 3 μm × 3 μm scans.)

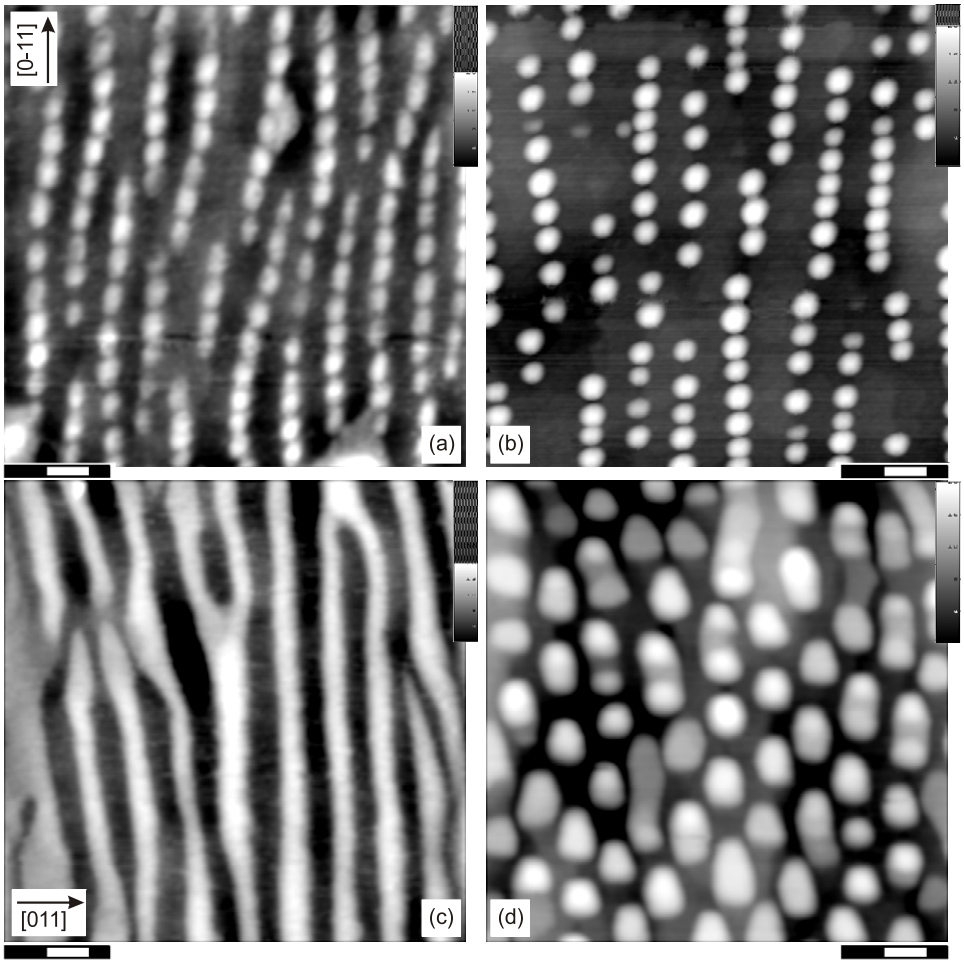

Figure 3. AFM images of $In_{0.5}Ga_{0.5}As$ ((a), (b)) and $In_{0.3}Ga_{0.7}As$ ((c), (d)) nano-features in multilayered structures grown using As_4 (left column) and As_2 (right column) gas fluxes. Horizontal scale bar corresponds to 250 nm, height gray-color scale corresponds to 20 nm.

direction) are equal for As_4 and As_2 fluxes (figure 2(e), curves 3 and 4). However, the spacing of the QD chains is larger for the case of As_2 flux (111 nm versus 83 nm in [011]). A similar trend is observed for multilayer structures in the perpendicular $[0\bar{1}1]$ direction where the QD spacing is larger for As_2-grown QDs in comparison with the As_4-grown ones (56 versus 44 nm). Therefore, we find that the difference in surface diffusion caused by the use of As_2 instead of As_4 coupled with the elastic strain fields that propagate between QD layers creates a significant difference in the resulting QD morphology after the growth of a QD superlattice. This allows us a degree of control over the lateral ordering of QDs in the self-assembly process and determining the final morphology of the superlattice InGaAs QD arrays.

We also analyzed the dependence of QD ordering on composition and nominal thickness of deposited wetting layer both for As_4 and As_2 fluxes. Figures 3 and 4 show AFM images of surfaces and high-resolution x-ray diffraction reciprocal space maps of our superlattice structures of $In_xGa_{1-x}As/GaAs$ where $x = 0.3$ for 15.5 MLs and $x = 0.5$ for 5.7 MLs. In each sample the GaAs spacer layer was 60 MLs. For each of these compositions the dot layers exceed the critical thickness for relaxation by 25%. As it is seen from figure 3, composition increasing from $x = 0.3$ to 0.5 leads to InGaAs nano-feature transformations from wire-like to closely packed dot-chains in the case of As_4 flux (figures 3(c) and (a)), and from large elongated QDs to small well separated QDs in the case of As_2 flux (figures 3(d) and (b)). The distances between nano-features in [011] and $[0\bar{1}1]$ surface directions determined by AFM and x-ray are shown in table 1. We should note that distribution width of measured distances was about ± 5 nm for AFM and ± 10 nm for x-ray investigations. X-ray data were extracted from the 004 and 113 x-ray reciprocal maps using common fitting procedures based on the dynamic theory of x-ray scattering [23–25]. Typical x-ray reciprocal space maps are shown in figure 4. There are clearly observed systems of satellite maxima corresponding to the vertical (central part) and the lateral (left and right maxima) periodicities in our structure. The lateral QD's spacing was determined for various azimuthal directions based on location measurements for lateral satellites on reciprocal maps. Slight inclination of the lateral satellites from the line perpendicular to the vertical satellites indicates vertical ordering of QDs that is inclined (2°–3°) to the sample surface normal, as was published in [26, 27].

Both AFM and x-ray data show a general decreasing of nano-features spacing in the [011] direction with increasing

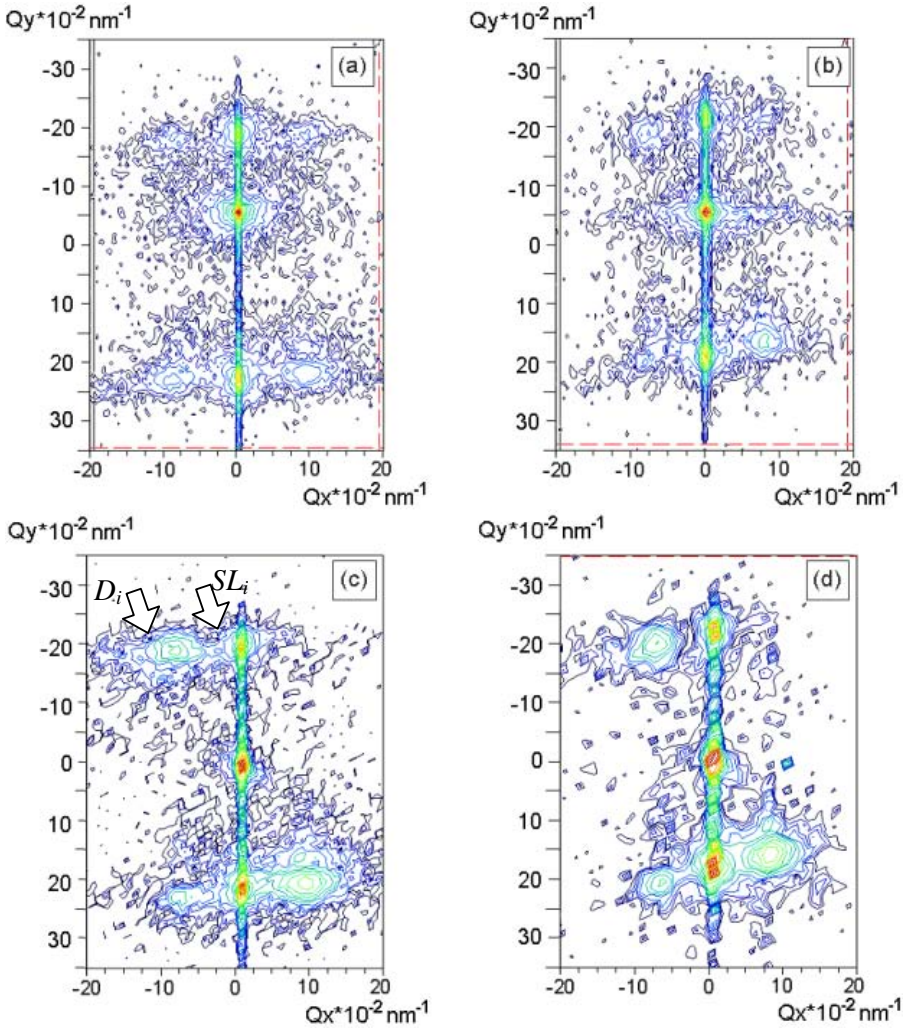

Figure 4. 004 ((a), (b)) and 113 ((c), (d)) reciprocal space maps of the $In_{0.5}Ga_{0.5}As/GaAs$ multilayer heterostructures grown with As_4 ((a), (c)) and As_2 ((b), (d)) fluxes. Conventional Cu Kα_1 x-ray source, diffraction plane is perpendicular to the [110] direction. Dot satellites D_i denotes the ith dot satellite along the Q_x direction centered on the SL_i multi-quantum well diffraction peak.

Table 1. X-ray and AFM data. For $x = 0.4$ AFM determined distances in [011] have FWHM of ± 5 nm (for cross-section line measurements) and ± 15 nm (for 2D FFT measurements). Note that small difference in absolute values between AFM and x-ray data explained by volume averaging in the case of x-ray.

	X-ray data QDs lateral distances, (nm)				AFM data QDs lateral distances, (nm)			
	As_4		As_2		As_4		As_2	
x	[011]	[0$\bar{1}$1]	[011]	[0$\bar{1}$1]	[011]	[0$\bar{1}$1]	[011]	[0$\bar{1}$1]
0.3	97	QWR-like[a]	97	Overlapped[b]	102	QWR-like	113	133
0.4	78	Overlapped	102	57	83	44	111	56
0.5	84	55.6	100	65.7	86	65	113	67

[a] 'QWR-like' denotes wire-like structure.

[b] 'Overlapped' denotes closely packed dot-chains with overlapped strain fields.

of In content in the case of As_4 flux (table 1) but a larger approximately constant QD spacing with change in In content for As_2 flux. Influence of flux composition and In content in $In_xGa_{1-x}As$ alloys on QD spacing is more significant in the orthogonal [0$\bar{1}$1] direction. In the case of $x = 0.3$ and As_2 flux, we have the largest QDs and largest spacing (figure 3(d)), while for As_4 flux there is a wire-like structure (figure 3(c)) For the $x = 0.4$, a spacing value difference is observed between As_4 and As_2 grown QDs (figures 2(c) and (d)). But, in the case of $x = 0.5$, the As_4 QD spacing in dot-chains ([0$\bar{1}$1] direction) is almost identical to the As_2 for these structures.

Certainly, the observed differences in QD ordering must be accompanied by changing in the deformation fields. We have estimated the typical deformation values for the GaAs

Table 2. Deformation values for GaAs spacer and InGaAs layers obtained from x-ray.

	Deformations $\varepsilon \times 10^{-3}$				Average vertical period of multilayer structure d, (nm)			QD's volume over 1 μm^2 $V \times 10^6$ nm^3 [a]		
	GaAs spacer		InGaAs layers							
x	As_4 $\varepsilon_{[011]}/\varepsilon_{[0\bar{1}1]}$	As_2 $\varepsilon_{[011]}/\varepsilon_{[0\bar{1}1]}$	As_4 $\varepsilon_{[011]}/\varepsilon_{[0\bar{1}1]}$	As_2 $\varepsilon_{[011]}/\varepsilon_{[0\bar{1}1]}$	Nominal	As_4	As_2	Nominal	As_4*	As_2*
0.3	1.75/1.75	1.51/1.51	20.0/18.0	20.0/20.0	21.3	22.6	23.2	4.38	0.90/21%	1.92/44%
0.4	1.85/1.85	1.85/1.85	20.0/19.0	17.0/17.0	19.4	19.9	20.0	2.40	1.06/44%	1.06/44%
0.5	1.71/1.48	1.41/1.16	19.2/17.5	18.4/17.0	18.6	18.5	18.8	1.61	0.39/24%	0.81/50%

[a] Columns show total volume of QDs over 1 × 1 μm^2 and relative difference between nominally deposited wetting layer volume and total volume of QDs in %.

spacer and InGaAs layers separately from corresponding x-ray measurements in [011] and [0$\bar{1}$1] directions (table 2). It was established that deformation in GaAs spacer layers is almost completely isotropic in the As_4- and As_2-grown structures (except for $x = 0.5$ structures). However, there is deformation anisotropy in As_4-grown InGaAs layers ($\varepsilon_{[011]} > \varepsilon_{[0\bar{1}1]}$). Here, we should note the isotropic deformation in the As_2 grown $In_xGa_{1-x}As$ for $x = 0.3$ and 0.4. Moreover, as can be seen from the x-ray data the deformation values are smaller in GaAs and InGaAs layers for As_2 grown structures in comparison with the As_4-grown ones. This is in general a result of the larger nanostructures that provide a greater amount of relaxation of the strain in the InGaAs layers.

The peculiarities described above regarding the surface morphology and the deformation fields are accompanied by different amounts of material involved in the nano-feature formation. We summarized the total volume of QDs using AFM data and compared it with the nominal volume of deposited InGaAs material (see table 2). This demonstrates that there is a nearly constant difference between the nominal and grown volumes of the nano-features in the case of As_2 flux for all the compositions of $In_xGa_{1-x}As$ layers, i.e., 44% from nominal, and that there is about half of that difference using As_4 flux. Note, that the total QD volume is the same for the As_4 and As_2 grown structures in the case of $x = 0.4$ at the same spacer deformations and average vertical period in both structures.

For the QD size distribution, we attribute all of the differences to differences in the surface diffusion lengths of In and Ga during growth with As_2 or As_4. If the diffusion length is small, there will be a high density of small dots, As_4. If the diffusion length is large, there will be a low density of large dots, As_2. In general, this holds true for the dot-chains and wires, i.e., a high density of dots in one direction can form a wire. These differences should not be confused with the differences resulting from composition change between different samples which are mainly due to the strain build up and relaxation in the InGaAs layers [28].

The strong PL in figure 5 demonstrates that with all of the studied changes in growth conditions we still attain a high quality QD superlattice capable of narrow linewidth exciton recombination. In general we find that the PL maxima, which is due to quantum confinement in the nanostructures, shifts to lower energy with increased In content as we would expect. However, since the confinement energy is strongly dependent

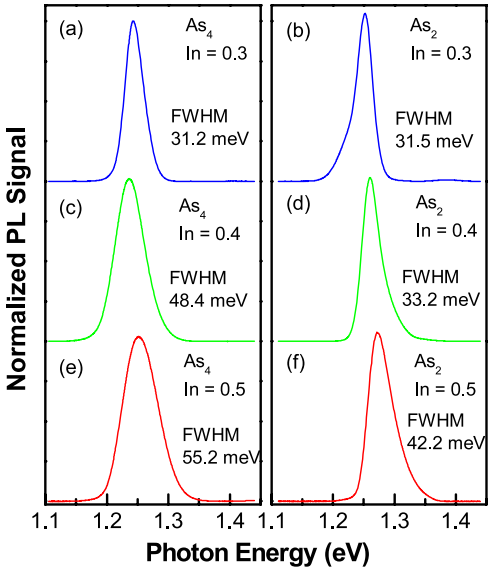

Figure 5. Low temperature ($T = 10$ K) normalized PL spectra of two sets of samples: (a), (c), (e)—grown using As_4 and (b), (d), (f)—grown using As_2. All PL spectra were taken using the same excitation density of 1 W cm^{-2}. The full-width at half-maximum (FWHM) is shown for each spectrum.

on the height of the nanostructure, we see some fluctuations in peak energy due to the shape of the nanostructure as grown under different conditions. These fluctuations are completely corroborated by AFM measurements.

The use of the As_2 background for effective manipulation of QD shape, positioning and deformations can be understood by considering surface diffusion. Due to the nature of the (2 × 4) GaAs(100) surface reconstruction, the adatoms diffusion length along [0$\bar{1}$1] direction is much larger in comparison with that for [011] direction [29].

This anisotropic surface diffusion leads to elongation of the QDs in each layer along the direction of higher mobility. This elongation in turn creates anisotropic strain fields in each capping layer (strain in the [0$\bar{1}$1] direction is smaller than in [011] [25]), which then enhances the elongation of the QDs subsequently forming chains or wires. The difference between the As_4 and As_2 appears to be in terms of limiting the ultimate diffusion lengths. A microprobe-RHEED/SEM study has shown that the lateral flow of Ga atoms is reduced under As_2 flux in comparison with As_4 [30]. Since the As_2

does not need to be cracked in order to incorporate into the crystal [31], having that as the arsenic source provides a lower energy barrier for incorporation and thus a shorter diffusion length for the adatoms [32]. This, as can be seen from the AFM images of figures 1 and 3 helps to keep the QDs as separate entities forming chains of QDs instead of wires.

4. Conclusions

Detailed AFM, x-ray and PL investigations of the QD self-directed ordering under As_4 and As_2 fluxes was curried out. It was established that due to differences in the adatom incorporation mechanisms from As_4 and As_2 fluxes the surface diffusion and deformation anisotropy are significantly different for samples grown using the different species. These facts provide new possibilities for precise governing of QD self-directed 3D ordering and improvement of their structural and optical properties.

Acknowledgments

The authors acknowledge the financial support of the NSF (through Grant DMR-0520550) and the Ministry of Education and Science of Ukraine (project M/175-2007).

References

[1] Bimberg D, Gruandmann M and Ledentsov N N 1999 *Quantum Dot Heterostructures* (New York: Wiley)
[2] Liu H C, Duboz J Y, Dudek R, Wasilewski Z R, Fafard S and Finnie P 2003 *Physica* E **17** 631
[3] Gutie'rrez M, Hopkinson M, Liu H Y, Herrera M, Gonza'lez D and Garcı'a R 2005 *Mater. Sci. Eng.* C **25** 793
[4] Phillips J 2002 *J. Appl. Phys.* **91** 4590
[5] Xie Q, Chen P and Madhukar A 1994 *Appl. Phys. Lett.* **65** 2051
[6] Rouvimov S, Liliental-Weber Z, Swider W, Washburn J, Weber E R, Sasaki A, Wakahara A, Furkawa Y, Abe T and Noda S 1998 *J. Electron. Mater.* **27** 427
[7] Ngo T T, Petroff P M, Sakaki H and Merz J L 1996 *Phys. Rev.* B **53** 9618
[8] Tersoff J, Teichert C and Lagally M G 1996 *Phys. Rev. Lett.* **76** 1675
[9] Leonard D, Krishnamorthy M, Reaves C M, Denbaars S P and Petroff P M 1993 *Appl. Phys. Lett.* **63** 3203
[10] Lee H, Johnson J A, Speck J S and Petroff P M 2000 *J. Vac. Sci. Technol.* B **18** 2193
[11] Nakamura Y, Schmidt O G, Jin-Phillipp N Y, Kiravittaya S, Muller C, Eberl K, Grabeldinger H and Schwizer H 2002 *J. Cryst. Growth* **242** 339
[12] Hyon C K, Choi S C, Song S H, Hwang S W, Son M H, Ahn D, Park Y J and Kim E K 2000 *Appl. Phys. Lett.* **77** 2607
[13] Mazur Yu I, Ma W Q, Wang X, Wang Z M, Salamo G J and Xiao M 2003 *Appl. Phys. Lett.* **83** 987
[14] Ma W Q, Hussein M L, Shultz J L and Salamo G J 2004 *Phys. Rev.* B **69** 233312
[15] Wang Z M, Churchil H, George C E and Salamo G J 2004 *J. Appl. Phys.* **96** 6908
[16] Chen W, Shin B, Goldman R S, Stiff A and Bhattacharya P K 2003 *J. Vac. Sci. Technol.* B **21** 1920
[17] Lytvyn P M, Strelchuk V V, Kolomys O F, Prokopenko I V, Valakh M Ya, Mazur Yu I, Wang Z M, Salamo G J and Hanke M 2007 *Appl. Phys. Lett.* **91** 173118
[18] Cirlin G, Tonkikh A, Ptitsyn V, Dubrovskii V, Masalov S, Evtikhiev V, Denisov D, Ustinov V and Werner P 2005 *Phys. Solid State* **47** 58
[19] Makoto I 2001 *Prog. Surf. Sci.* **66** 53
[20] Sugaya T, Amano T and Komory K 2006 *J. Appl. Phys.* **100** 063107
[21] Sugaya T, Furue S, Amano T and Komory K 2007 *J. Cryst. Growth* **301/302** 801
[22] Foxon C T and Joyce B A 1981 *Current Topics in Materials Science* vol 7, ed E Kaldis (Amsterdam: North-Holland)
[23] Beresford R and Xu J M 2005 *Appl. Phys. Lett.* **86** 206102
[24] Springholz G, Holy V, Pinczolits M and Bauer G 1998 *Science* **282** 734
[25] Wang Z M, Holmes K, Mazur Yu I and Salamo G J 2004 *Appl. Phys. Lett.* **84** 1931
[26] Grigoriev D, Schmidbauer M, Schäfer P, Besedin S, Mazur Yu I, Wang Z M, Salamo G J and Köhler R 2005 *J. Phys. D: Appl. Phys.* **38** A154
[27] Schmidbauer M, Seydmohamadi S, Grigoriev D, Wang Z M, Mazur Yu I, Schäfer P, Hanke M, Köhler R and Salamo G J 2006 *Phys. Rev. Lett.* **96** 066108
[28] Chang L L and Ploog K 1985 *Molecular Beam Epitaxy and Heterostructures* (Dordrecht: Martinus Nijhoff)
[29] Kladko V P, Strelchuk V V, Kolomys O F, Slobodian M V, Mazur Yu I, Wang Z M, Kunets Vas P and Salamo G J 2007 *J. Electron. Mater.* **36** 1555
[30] Ogura T, Kishimoto D and Nishinaga T 2001 *J. Cryst. Growth* **226** 179
[31] Morgan C G, Kratzer P and Scheffler M 1999 *Phys. Rev. Lett.* **82** 4886
[32] Sugaya T, Komori K, Yamauchi S and Amano T 2005 *J. Vac. Sci. Technol.* B **23** 1243